



## SAR remote sensing for monitoring harmful algal blooms using deep learning models

Kritnipit Phetanan, Do Hyuck Kwon, Jinmyeong Lee, Heewon Jeong, Gibeom Nam, Euiho Hwang, JongCheol Pyo & Kyung Hwa Cho

To cite this article: Kritnipit Phetanan, Do Hyuck Kwon, Jinmyeong Lee, Heewon Jeong, Gibeom Nam, Euiho Hwang, JongCheol Pyo & Kyung Hwa Cho (2025) SAR remote sensing for monitoring harmful algal blooms using deep learning models, GIScience & Remote Sensing, 62:1, 2524202, DOI: [10.1080/15481603.2025.2524202](https://doi.org/10.1080/15481603.2025.2524202)

To link to this article: <https://doi.org/10.1080/15481603.2025.2524202>



© 2025 The Author(s). Published by Informa UK Limited, trading as Taylor & Francis Group.



[View supplementary material](#)



Published online: 18 Jul 2025.



[Submit your article to this journal](#)



Article views: 2326



[View related articles](#)



[View Crossmark data](#)



Citing articles: 1 [View citing articles](#)

# SAR remote sensing for monitoring harmful algal blooms using deep learning models

Kritnipit Phetanan<sup>a\*</sup>, Do Hyuck Kwon<sup>a\*</sup>, Jinmyeong Lee<sup>b</sup>, Heewon Jeong<sup>c</sup>, Gibeom Nam<sup>d</sup>, Euiho Hwang<sup>d</sup>, JongCheol Pyo<sup>e</sup> and Kyung Hwa Cho<sup>f</sup>

<sup>a</sup>Department of Civil Urban Earth and Environmental Engineering, Ulsan National Institute of Science and Technology, Ulsan, Republic of Korea; <sup>b</sup>Environmental Engineering, Chungnam National University, Daejeon, Republic of Korea; <sup>c</sup>Future and Fusion Lab of Architectural, Civil and Environmental Engineering, Korea University, Seoul, The Republic of Korea; <sup>d</sup>Water Resources Satellite Center, K-water Research Institute, Daejeon, Republic of Korea; <sup>e</sup>Department of Environmental Engineering, Pusan National University, Busan, Republic of Korea; <sup>f</sup>School of Civil, Environmental and Architectural Engineering, Korea University, Seoul, Republic of Korea

## ABSTRACT

Harmful Algal Blooms (HABs) threaten aquatic ecosystems, necessitating effective monitoring strategies in water resource management. Satellite-based remote sensing has emerged as a popular method to address the limitations of in-situ monitoring. However, cloud covers can obstruct optical imagery, causing data loss. Synthetic Aperture Radar (SAR) imagery, with its capabilities, can penetrate through any weather conditions. We applied SAR imagery with the Faster Regional Convolutional Neural Networks (Faster R-CNN) model to detect the algal bloom. The dataset of the Geum River Basin was obtained from 2020 to 2022. The sigma naught values (dB) were analyzed from the SAR imagery to clarify the reflectance properties of algae in VH and VV polarizations. The values ranged between  $-12$  dB and  $-33$  dB and  $-5$  dB and  $-27$  dB for VH and VV polarization, respectively. The model was developed with hyperparameter optimization to detect the algal bloom by splitting the training from 2020 to 2022, and the testing dataset 2022. Evaluation metrics including precision, recall, and F1 scores yielded values of 0.600, 0.692, and 0.643, respectively. The developed model was simulated to identify the seasonal outbreak. The result illustrated that the algal blooms were detected only in the summer of 2021 and 2022. Furthermore, the model was validated in supporting an existing algal alert report, demonstrating the potential for real-time monitoring. Finally, this study highlights the effectiveness of employing SAR imagery with the Faster R-CNN model to develop an algorithm for detecting algal blooms, offering advancements in water management practices.

## ARTICLE HISTORY

Received 4 January 2025  
Accepted 19 June 2025

## KEYWORDS

Harmful algal blooms; remote sensing; synthetic aperture radar; deep learning; object detection; faster regional convolutional neural network

## 1. Introduction


The global concern of irregularly increasing harmful algal blooms (HABs), particularly cyanobacterial blooms in South Korea, has posed significant challenges to aquatic ecosystems (Kim, Cha, and Cho 2024). HABs obstruct sunlight and lead to fluctuations in nutrients and dissolved oxygen levels, directly impacting aquatic life and contributing to water quality degradation, which could have implications for water resource management (Kwon, Hong, Abbas, Pyo, et al. 2023). In addition to the degradation of water quality directly caused by HABs, the toxins they produce can also have an adverse impact on routine water quality monitoring (Brooks et al. 2016). Algae monitoring is essential for ensuring clean water access, maintaining water quality and environmental indicators for informed decision-making and

sustainable practices (Qian et al. 2024; Qiu et al. 2023). Although informative, traditional in-situ procedures, such as direct sampling come with substantial time, labor, and cost requirements, as they are conducted at specific times and locations (Baek et al. 2022). This can limit the spatial coverage and frequency of data collection, potentially missing critical variations in water quality over time and space (Foster et al. 2019). Therefore, algae monitoring highlights the need for complementary approaches to comprehend algal bloom dynamics.

Remote sensing techniques are utilized as an alternative method to overcome the limitations of traditional in-situ monitoring, gaining popularity for their effectiveness in acquiring information without physical contact (Cook et al. 2023; Kim et al. 2020). Satellite-based remote sensing, particularly through the MultiSpectral

**CONTACT** JongCheol Pyo  [jongcheol.pyo@pusan.ac.kr](mailto:jongcheol.pyo@pusan.ac.kr); Kyung Hwa Cho  [khcho80@korea.ac.kr](mailto:khcho80@korea.ac.kr)

\*Co-first authors: Kritnipit Phetanan, Do Hyuck Kwon.

 Supplemental data for this article can be accessed online at <https://doi.org/10.1080/15481603.2025.2524202>

© 2025 The Author(s). Published by Informa UK Limited, trading as Taylor & Francis Group.

This is an Open Access article distributed under the terms of the Creative Commons Attribution-NonCommercial License (<http://creativecommons.org/licenses/by-nc/4.0/>), which permits unrestricted non-commercial use, distribution, and reproduction in any medium, provided the original work is properly cited. The terms on which this article has been published allow the posting of the Accepted Manuscript in a repository by the author(s) or with their consent.

Instrument (MSI) on Sentinel-2, has been instrumental in monitoring algal blooms by capturing imagery across multiple spectral bands, thereby facilitating detailed water quality analyses (Kwon et al. 2023). Steinhausen et al. (2018) demonstrated that the impact of weather conditions might cause difficulties in visible satellite imagery. For this reason, Synthetic Aperture Radar (SAR) imagery has been introduced in marine research for wetland monitoring, and flood detection, especially beneficial in areas where data is limited (Niculescu et al. 2020). Operating in the microwave spectrum, SAR can penetrate cloud cover, making it valuable when the MSI is hindered by atmospheric conditions. Previous studies have utilized SAR imagery to interpret various water quality parameters, such as salinity (Shareef, Toumi, and Khenchaf 2016). However, algae detection through SAR is rarely observed due to the difficulty in complex interpretation using traditional empirical calculation methods, leading to notable errors (Raj, Sethunadh, and Aparna 2016). Utilizing a data-driven model, a computer-based technique, to interpret and analyze can offer a more reliable approach and time-saving consumption.

A data-driven model has been utilized to manage water resources by predicting the targets to get ready with the mitigation procedure (Jo et al. 2020). On the other hand, mathematical-based models were limited in terms of the reliability of predefined equations and assumptions (Manteaux et al. 2023). Faster Regional Convolutional Neural Networks (Faster R-CNN), one of the data-driven models, have been introduced to address these challenges (Solomatine, See, and Abrahart 2009). The model can detect objects by extracting image features and training the relationships between the input and output datasets, without relying on predefined equations (Fang et al. 2020). It has been employed for object detection in hydrology and remote sensing applications based on its capabilities (Evora and Coulibaly 2009). Chai et al. (2021) applied the Faster R-CNN model to detect ship-like targets from SAR imagery and effectively realized the objects. Despite this, few researchers have applied the data-driven model with SAR imagery to detect algal blooms, which are currently a major cause of the deteriorating water quality (Wu et al. 2019). Therefore, developing the Faster R-CNN model for detecting the outbreak of algal bloom from SAR imagery holds the potential to contribute to sustainable water resources and mitigation efforts.

In summary, this study presents a novel algorithm by integrating SAR remote sensing data with a data-driven model to detect algal blooms, offering enhanced insights into their occurrence. The research aimed to

achieve three main objectives: first, to analyze SAR backscatter values to observe how algal blooms reduce surface roughness, resulting in diminished backscatter and dark patches in SAR images and to clarify the correlation between these patterns and algal bloom presence. Second, we developed a deep learning-based detection model that uses SAR imagery as the primary feature input and visible satellite imagery as ground truth, capitalizing on SAR's unique backscattering characteristics to accurately identify algal blooms. Finally, we applied this model to identify seasonal outbreaks and detect existing blooms under adverse weather conditions, providing a reliable alternative when optical satellite imagery is obstructed by cloud cover. This demonstrates its effectiveness in supporting existing algal alert systems.

## 2. Materials and methods

### 2.1. Research overview

This research was conducted through a comprehensive three-step process, encompassing data acquisition, data preparation, and applying deep learning techniques, as illustrated in Figure 1. The Sentinel-1 SAR C-band was acquired as the main input dataset, while the Sentinel-2 MSI data was utilized as ground truth, respectively, as shown in Figure 1(a). Subsequently, as stated in Figure 1(b), we extracted the sigma naught values in both Vertical–Vertical (VV) and Vertical–Horizontal (VH) polarizations from SAR imagery, while MSI imagery was used to identify the geographic coordinates indicative of the algal bloom. Waterbodies extracted from the SAR imagery were utilized to obtain hydraulic information. Then, we combined three layers of VV, VH, and waterbody, generating the input dataset. Data augmentation techniques, including rotation, and flipping were employed to enhance the dataset before utilizing it as input features for the algal bloom detection model. In Figure 1(c), the algal blooms were analyzed by plotting the sigma naught values reflected from SAR imagery. Following that, the algal detection model was developed using the Faster R-CNN model with hyperparameter optimization methods, employing the SAR imagery dataset as input features to train and aiming to predict the blooms. The evaluated models, both trained and tested, were assessed using a confusion matrix, which serves as a performance measurement for machine learning classification. This involved comparing the simulated outcomes with MSI imagery visually, serving as ground truth data. In addition to research assessments, the study further discussed the seasonality of algal blooms and their correlation with environmental parameters. Our model was

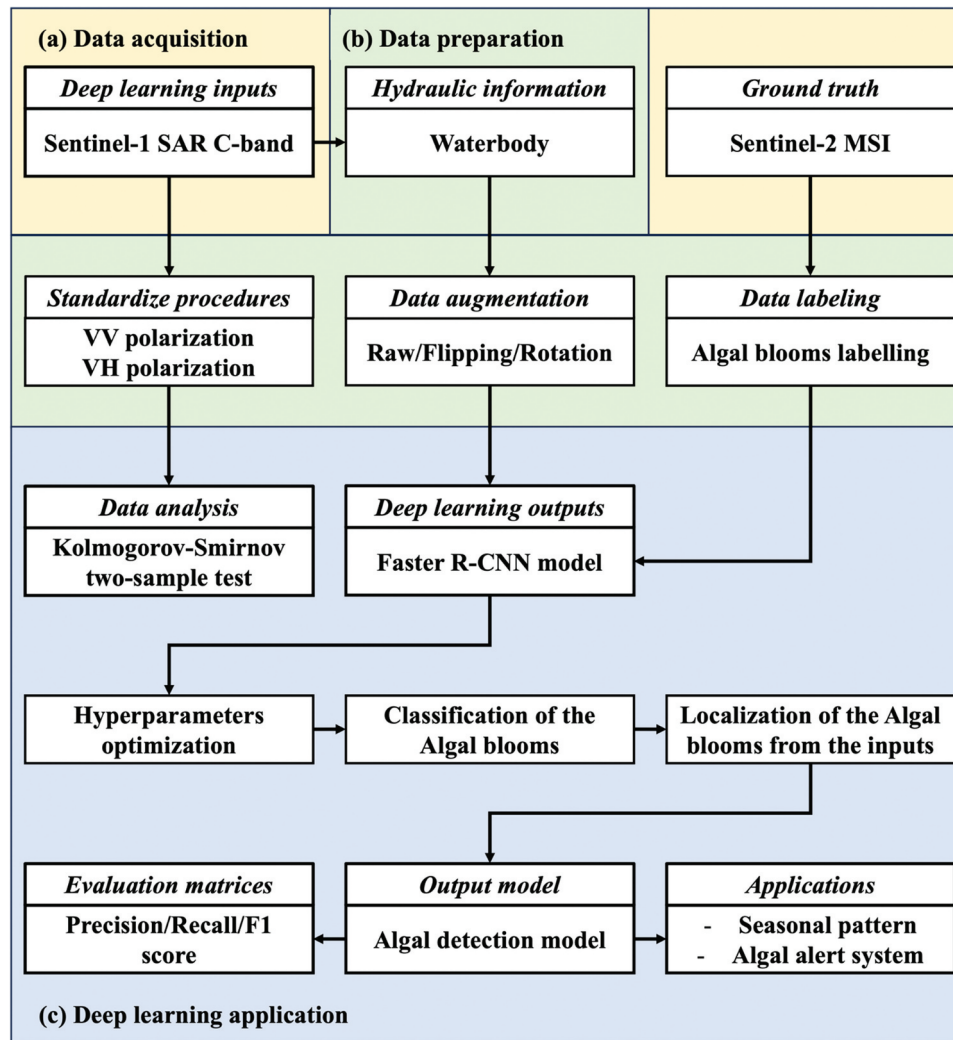


**Figure 1.** The research flow chart illustrates the algal bloom detection model using a deep learning-based approach with SAR C-band imagery: (a) data acquisition for deep learning inputs and ground truth, (b) data preparation, including SAR imagery standardization, algal bloom labeling, and waterbody extraction, and (c) application of the deep learning model for algal bloom detection.

implemented on a system equipped with a 13th Gen Intel(R) Core(TM) i9-13900F 2.00 GHz processor, 64 GB of DDR5 RAM, and an NVIDIA GeForce RTX 4090 graphics card.

## 2.2. Study area

The Geum River (GR), one of the four largest rivers in South Korea, is situated in the mid-western region (N 36.35°–36.52°, E 127.48°–127.60°). GR spans 396.4 km and encompasses a basin area of approximately 9914.02 km<sup>2</sup> (Kim, Muhammad, and Maeng 2016). GR grants a significant amount of water resources for municipal, domestic, agricultural, and industrial. Moreover, the basin is characterized by the monsoon, marked by periods of heavy rainfall (Jung et al. 2019). Over the past three decades, the recorded annual temperature and precipitation from June to August averaged 10.9°C and 1,295 mm,

respectively (Kwon, Hong, Abbas, Park, et al. 2023). This caused GR to receive approximately 6.4 tons of freshwater discharges annually (D. Kim et al. 2022). However, the construction of dams along the GR has disrupted the natural flow of freshwater into the Yellow Sea estuary, leading to altered water dynamics, stagnant conditions, and the occurrence of algal blooms (Shim, Yoon, and Yoon 2018). HABs have broken out annually in the GR basin (Park 2012). Especially, at the reservoir called Daecheong Reservoir located in the GR basin is the focus source of the outbreak of algae (Back, Park, and Park 2015). Daecheong Reservoir is one of the key areas of focus in government reports because it is one of the main sources of residential, agricultural, and industrial purposes in South Korea (Srivastava et al. 2015). These challenges arise from the influx of both non-point and point source pollution, driven by intense runoff and industrial or agricultural complexes (S. Kim et al. 2022). In our study, we

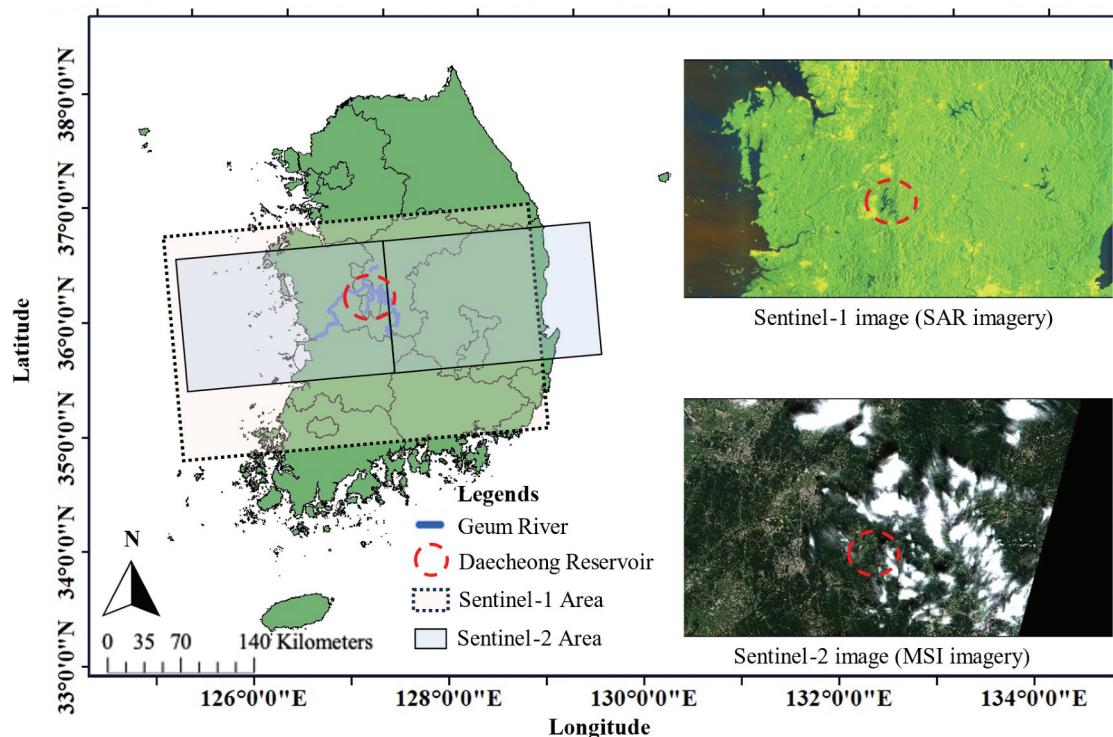


**Figure 2.** Study coverage: Geum River basin along with its legends and Sentinel-1, and Sentinel-2 coverage acquisition zone.

selected the GR basin, focusing on the Daecheong Reservoir as the representative region, depicted in Figure 2.

### 2.3. Data Processing

In the study, the research methodology heavily relied on diverse datasets, encompassing SAR imagery, which is detailed in Table S1, and waterbody extraction imagery as the input datasets. Initially, a resolution of 10 m from SAR C-band imagery was sourced from the European Space Agency (ESA, <https://dataspace.copernicus.eu/>) (Ecosystem 2023). SAR imagery, a remote sensing technology employed by the Sentinel-1 observation satellite, enables the generation of high-resolution imagery regardless of cloud cover or illumination, even during day or nighttime under all weather conditions (Fletcher and European Space Agency 2012). The Sentinel-1 satellite, operating within a frequency range of 5.3 GHz to 5.8 GHz, orbits at an altitude of 693 km (Moeller et al. 2010).

To enhance our analysis, hydraulic information – geospatial datasets that offer insights into the physical characteristics and behavior of waterbodies and their surrounding environments – is essential for accurately detecting and monitoring algal blooms. This facilitates the precise identification of waterbodies, ensuring algal bloom detection is confined to relevant aquatic areas. Utilizing waterbody

extraction techniques with SAR imagery and deep learning methods enhances model accuracy and supports targeted mitigation strategies (Kim et al. 2021). From the Sentinel Application Platform (SNAP) program, VV and VH polarizations were extracted from the SAR imagery through seven processing steps, including: 1. Apply Orbit File, 2. Thermal Noise Removal, 3. Radiometric Calibration which is used to convert digital numbers to sigma naught (backscatter coefficients), 4. Speckle Filtering, 5. Terrain Correction, 6. Subset, subsequently, 7. Conversion to decibels (dB) (Filipponi 2019). The sigma naught ( $\sigma^0$ ) or backscatter coefficients represent the radar backscatter coefficient normalized by the ground area, indicating the amount of energy returned to the sensor. This effect is influenced by surface roughness, moisture content, and geometry. To ensure temporal independence and avoid overestimation of model accuracy due to spatial-temporal autocorrelation, a time-based split was employed over 3 years (July 2020–September 2022), the dataset included 5080 images from 21 July 2020 to 9 September 2022 for training and 1200 images from 9 September 2022 for testing, with data augmentation applied to enhance variability (Appendix A).

In addition to SAR data, the Sentinel-2 satellite was instrumental in precisely locating the spatial coordinates of algal blooms when used alongside SAR imagery. Only Sentinel-2 images acquired on the same dates as the corresponding Sentinel-1 imagery were selected for analysis. This combined dataset

facilitated a performance evaluation by comparing results with simulated outputs. Sentinel-2's multi-spectral sensor, with a 10-m resolution, complemented SAR data by capturing imagery across 13 optical bands (ESA 2013), although we focused on the Normalized Difference Chlorophyll Index (NDCI) and three optical bands (blue, green, and red) for analysis (Appendix B). This combined dataset facilitated a performance evaluation by comparing results with simulated outputs.

Along with remote sensing data, daily environmental parameters were gathered from July 2021 to September 2022 to analyze the seasonal outbreak relationship of blooms in section 3.3.1 Parameters including water temperature ( $^{\circ}\text{C}$ ), chlorophyll-a ( $\text{mg}/\text{m}^3$ ), and dissolved oxygen (DO) ( $\text{mg}/\text{L}$ ) were obtained from the National Institute of Environmental Research (NIER, <http://211.114.21.27/web>.) (National Institute of Environmental Research 2023). These parameters offered insights into the seasonal dynamics of algal blooms (Ji et al. 2017; Raven and Geider 1988; Sterner and Grover 1998; H. Zhang et al. 2021).

## 2.4. Deep learning approach

The Faster Regional Convolutional Neural Network (Faster R-CNN) model, based on Convolutional Neural Network (CNN) (Appendix C), was introduced as the

object detection deep learning approach (Ren et al. 2015). The objective is to train the model to acquire proficiency in both object recognition and localization within the images. The model consists of three main steps to detect objects by classifying many regions; The extraction of features, Region Proposal Network (RPN), and Region-based Convolutional Neural Network (R-CNN) as shown in Figure 3 (Lee, Kim, and Kyeong 2016). In our study, Figure 3(a) illustrates the overall architecture of the faster R-CNN model. The pre-processed imagery undergoes CNN processing, utilizing the Residual Networks (ResNet) 50 architecture to produce feature maps. Feature extraction is utilized in image classification to extract outstanding features from images, as established in prior research (Krizhevsky, Sutskever, and Hinton 2012). Studies have also demonstrated that incorporating hydraulic information into CNNs has proven effective for waterbody detection and segmentation (Z. Zhang et al. 2021).

In Figure 3(b), RPN, a vital component of the Faster R-CNN, significantly contributes to the model's efficiency and precision in recognizing various areas (Jiang and Learned-Miller 2017). It operates as a CNN generating a set of rectangular object proposals within an image. Each rectangle is assigned a score indicating its likelihood of containing an object, called a region of interest (Rois) (Sun, Wu, and Hoi 2018). The scores generated in this process contribute to the generation of bounding

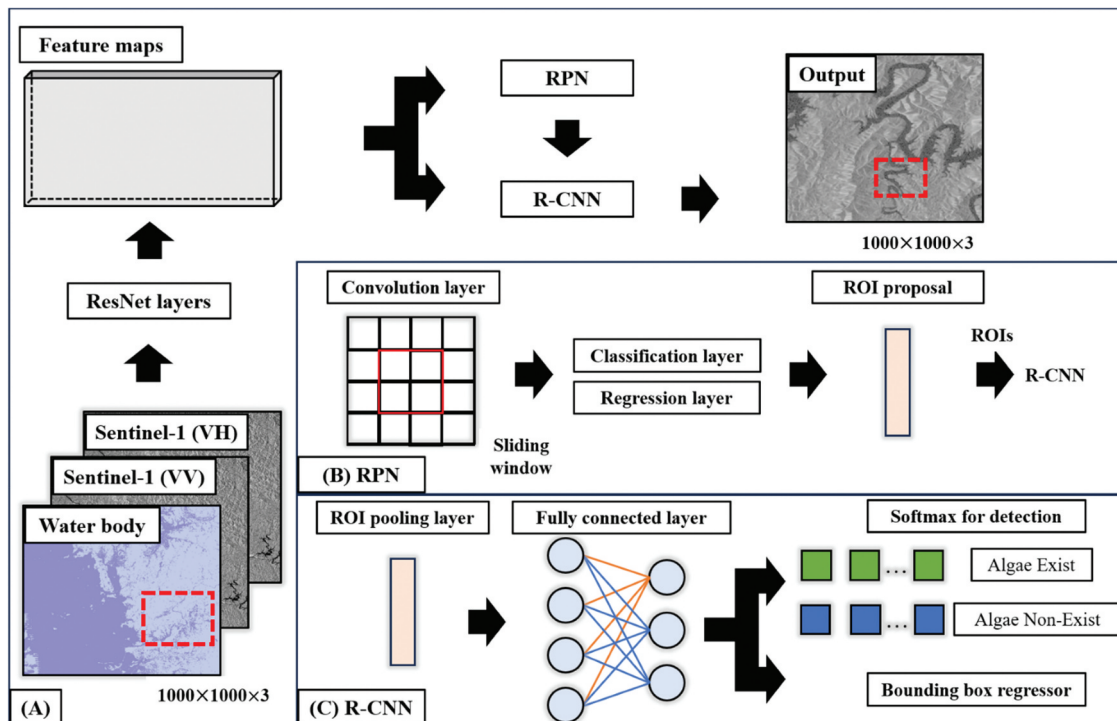


**Figure 3.** Faster R-CNN model architectures for algal detection; (a) showed the overall architectures namely the main input and output data, and the model's unique characteristics (b) indicated region proposal network, explaining its operational mechanism (c) elucidated regional CNN, offering insights into its role for the algal bloom detection.

boxes, offering a comprehensive understanding of the algal bloom dynamics within the imagery. Subsequently, in Figure 3(c), Rols undergo classification, and their boxes are regressed (Girshick 2015). The pooling features passed through the hidden fully connected layers to obtain bounding boxes with scores, detecting the existence or absence of algal bloom.

The bounding box sizes were determined by analyzing the spatial extent of algal blooms identified using the NDCI from Sentinel-2 imagery. This process involved manually comparing NDCI-derived bloom areas with corresponding SAR imagery to establish bounding boxes that accurately encompass the observed blooms. This approach follows the methodology described in Gernez et al. (2023), where visual interpretation was used to delineate bloom areas. However, this manual approach is subject to potential errors and limitations, such as discrepancies between optical and SAR data due to differing sensor characteristics and environmental conditions. These factors may introduce uncertainties in bounding box dimensions, potentially affecting the model's detection accuracy. Acknowledging these limitations is crucial for interpreting the model's performance and highlights the need for further refinement in bounding box determination methods (N.Zhang et al. 2021).

We also acknowledge that AI models often lack interpretability and transparency. Explainable Artificial Intelligence (XAI) addresses these issues by making AI systems more understandable, which is crucial as AI applications expand into critical domains. In the future work, we plan to integrate XAI techniques to enhance our model's interpretability, thereby improving trust and effectiveness in detecting algal blooms (Letrache and Ramdani 2023).

In our study, we optimized the model to minimize loss and maximize predictive accuracy, recognizing that even minor variations in hyperparameter configuration can significantly impact the efficiency of algal bloom detection (Lakhmiri, Digabel, and Tribes 2021). We conducted using the grid search method to enhance model performance as listed in Table S2 (Bergstra, Ca, and Ca 2012). The hyperparameters including learning rate, weight decay, batch size, epoch, and optimizer were defined. The learning rate determines the step size at each iteration to reach a minimum loss (Alibrahim and Ludwig 2021). Weight decay is used to regularize the weight update in the Faster R-CNN (Goodfellow, Bengio, and Courville 2016). Batch size is the division of the dataset into smaller parts and passes through the algorithm, while epoch is the entire dataset passed forward and backward (Smith et al. 2017). An optimizer is applied to optimize the algorithms and minimize an error function (Hammad Saleem et al. 2020).

The model underwent training for 150 epochs on the designated training set. Adam served as the optimizer, with an initial learning rate ranging from 0.000001 to 0.01, while the weight decay ranged from 0.0 to 0.9. The batch size was set to be in the ranges of 2–32, creating a data loader where each training batch consists of a sample.

## 2.5. Model evaluation

The assessment of the Faster R-CNN model's quality and effectiveness is facilitated through the utilization of various evaluation tools, comparing simulated values against ground truth through various techniques. The following tool called a confusion matrix was utilized to offer valuable insights into the performance of algal bloom detection models of a classification model including Precision, Recall, and F1-score (Junker, Hoch, and Dengel 1999; Y. K. Kim et al. 2022). First, precision focuses on the relevance of the positive predictions made by a model. A higher precision value means that the number of correct positive predictions of algae from the model makes fewer false positive predictions relative to the total positive predictions. Recall is the sensitivity of the model and is crucial in situations where missing a positive occurrence has a significant outcome. A higher recall value shows that the model effectively identifies a larger number of positive occurrences of algal bloom. The F1 score uses the combination of precision and recall, providing a balanced evaluation of the imbalanced model's performance in the dataset. A higher F1 score determines the accurate identification of both true positives and true negative cases. These evaluation metrics were calculated as follows:

$$Precision = \frac{TP}{(TP + FP)} \quad (1)$$

$$Recall = \frac{TP}{(TP + FN)} \quad (2)$$

$$F1score = 2 \times \frac{Precision \times Recall}{Precision + Recall} \quad (3)$$

Where  $TP$  are true positives, both simulated results and ground truths showed the existence of algae correctly,  $TN$  are true negatives, both simulated results and ground truths showed the nonexistence of algae correctly,  $FP$  are false positives which mean the simulated imagery resulted in the existence of algae but the ground truths showed no existence of algae, and  $FN$  are false negatives, which mean the simulated imagery resulted in the nonexistence of algae, but there is an existence of algae in the ground truths.

### 3. Results and discussions

#### 3.1. Algal bloom distribution analysis by utilizing SAR imagery

Our study extracted SAR imagery through standardized procedures, and sigma naught values were computed for both VH and VV polarizations. Figure 4 illustrates the distribution of algal blooms, vegetation, and water features by colors in terms of sigma naught values and algal pixel density. The algal bloom, vegetation, and water were colored orange, green, and blue, respectively. Figure 4(a,b) independently presented the VH and VV polarizations. According to the figure, the analysis revealed that reflectance values for algal blooms approximately ranged between  $-12$  dB and  $-33$  dB for VH polarization and  $-5$  dB and  $-27$  dB for VV polarization. Concurrently, vegetation predominately exhibited data distribution between  $-10$  dB and  $-21$  dB and  $-3$  dB and  $-15$  dB, while water distribution ranged between  $-21$  dB and  $-34$  dB and  $-15$  dB and  $-28$  dB for VH and VV polarizations, respectively. The sigma naught values, representing the radar backscatter intensity from surface targets, have been widely used in prior research as a reference for classifying aquatic surface features, including algal blooms (Parmuchi, Karszenbaum, and Kandus 2002). These values are particularly useful in identifying changes in surface roughness, often caused by dense algal accumulations. We analyzed the algal blooms in the GR basin using SAR imagery to quantify the reflectance values of the algal bloom from the radar signal to the sensor. To establish these class boundaries, only the locations where algal blooms were seen from SAR and analyzed using NDCI from MSI imagery were chosen by visual interpretation, as demonstrated in Figure 5 (Appendix D). Only co-located observations

from images acquired on the same date were used to ensure temporal consistency. The sigma naught values for each algal bloom spot were accumulated from the acquired dataset, and the overall graph was plotted.

The analysis indicated distinctive peaks for each feature, signifying unique reflectance properties. However, mixed pixels existed in all remote sensing imagery due to image resolution, with coarser imagery leading to more mixed pixels would be found (Adams, Smith, and Johnson 1986). Both VH and VV polarizations exhibited overlapping bins, particularly in the distribution data of algal blooms, which showed two peaks. To determine whether algal blooms share distributions with vegetation and water, we applied the Kolmogorov–Smirnov two-sample test (KStest2) (Appendix E) (Massey 1951). Through the KStest2 analysis, we found that one peak representing algal blooms aligned with water features, indicating that algal blooms were captured alongside water features. Inoue, Sakaiya, and Wang (2014) demonstrated water features approximately  $-28.5$  dB for VH and  $-21.1$  dB for VV polarization, validating the analysis. However, the similarity in backscatter signatures between algal blooms and other surface features, such as vegetation, necessitates further verification to accurately distinguish between them. Relying solely on statistical distribution analysis may be insufficient, as environmental factors like wind speed and water surface conditions can introduce irrelevant features, potentially leading to skewed conclusions. For instance, low wind speeds can cause smooth water surfaces, resulting in dark regions in SAR images that may be misinterpreted as algal blooms (Wu et al. 2018). To enhance the accuracy of algal bloom detection in SAR imagery, integrating optical remote sensing data is advisable. This integration provides complementary spectral

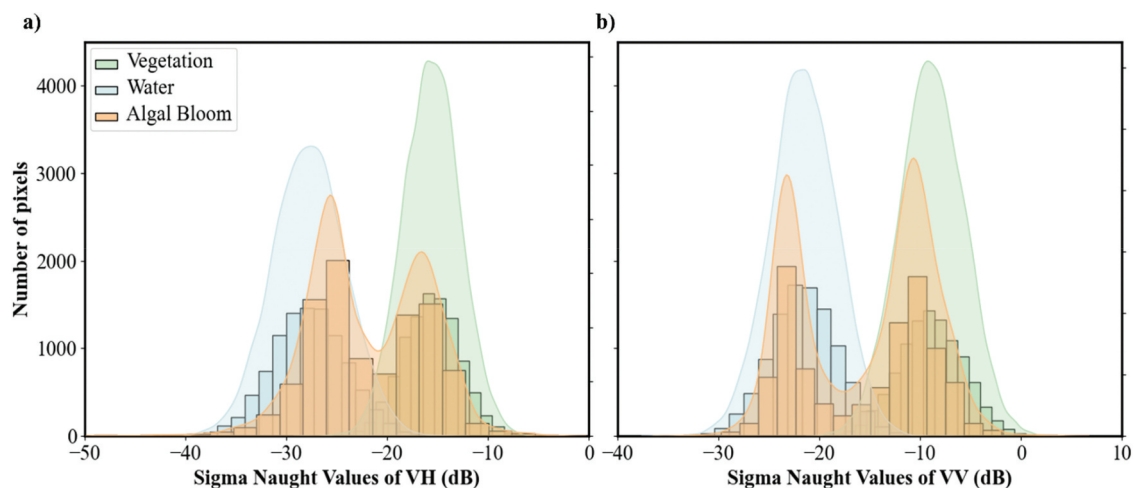


**Figure 4.** The data distribution of the algal bloom in the SAR imagery from the Guem River showed the comparison with other substances namely vegetation, and water. (a) Sigma naught values of VH polarization (b) Sigma naught values of VV polarization.

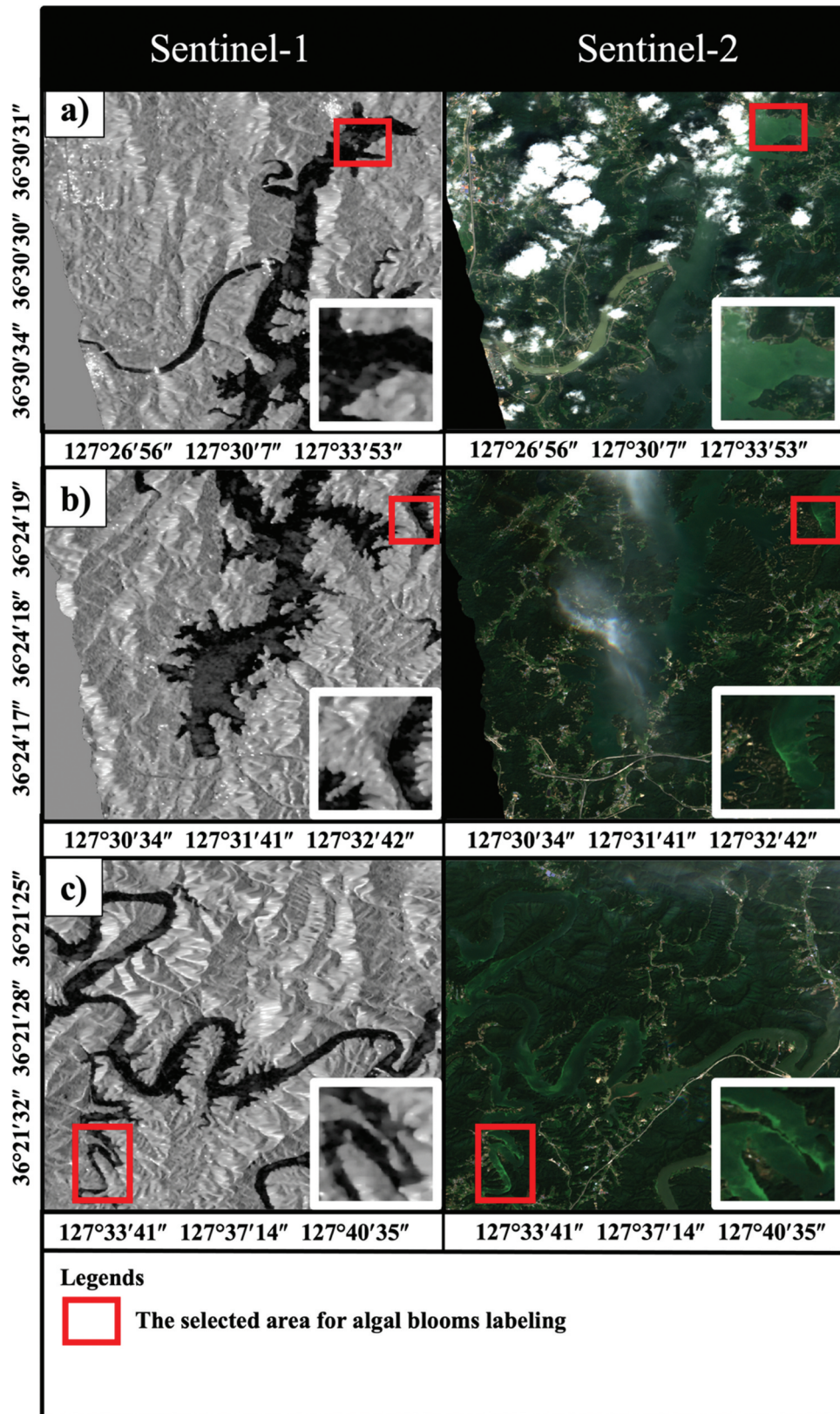


**Figure 5.** Representative sample areas selected for data distribution analysis. Each location is shown with its corresponding acquisition date. (a) Mooni intake area (August 25, 2020), located in the northwestern part of Daecheong Lake. (b) Hoenam (September 9, 2022), located in the central part of the lake. (c) So-oak Cheon (September 9, 2022), located in the southern-central part of the lake. Each location is represented by a pair of Sentinel-1 (SAR) and Sentinel-2 (optical) images acquired on the same date.

information that can confirm the presence of algal blooms, thereby addressing the limitations inherent in SAR data alone. Studies have demonstrated that combining SAR and optical data improves the monitoring of algal blooms by leveraging the strengths of both data types (Adamo et al. 2013). Additionally, understanding the characteristics of SAR signals is crucial, as they are influenced by factors like surface roughness and dielectric properties, which can affect backscatter intensity and complicate interpretation.

### 3.2. Performance evaluation of algal bloom detection model

To identify the occurrence of algal blooms, an effective data-driven model was employed to detect differences between algal blooms and non-algae (Khan et al. 2021). We developed the Faster R-CNN model to detect the algal bloom in the GR basin from SAR imagery. The dataset was split into a training set comprising 5080 images and a testing set comprising 1200 images. The grid searching method was conducted for hyperparameter optimization to improve model performance as listed in Table S2. Learning rate, batch size, and weight decay were selected from the configured ranges as the optimal model parameters which were 0.0001, 32, and 0.0, respectively. These parameters were the best parameters for having the minimum error rate. Jiang and Xu (2022) demonstrated that hyperparameter optimization strongly influenced the model and improved the simulated performances. The classification score threshold was set to be greater than 0.7 (Li, Qu, and Shao 2017). Figure 6 illustrates detection results post-hyperparameter optimization, showcasing instances such as an algal bloom in Mooni on 25 August 2020, within the Daecheong Reservoir (Figure 6(a)). Similarly, Figure 6(b,c) showed detection results from Choodong on 25 August 2020, and So-oak Cheon on 14 September 2022, both in territorial waters of the Daecheong Reservoir. These locations are prone to algal blooms due to their slow water flow and high retention time, typical of closed-water systems (J. Kim et al. 2023). Wang et al. (2022) conducted a study that showed a well-validated object detection model through the utilization of SAR imagery. Specifically, the simulation result from Figure 6(c) was from the testing dataset which even proved the model's potential.

As detailed in Table 1, evaluation metrics were employed to assess the performance of the algal bloom detection from the Faster R-CNN model. These metrics were applied to both the training and testing

datasets, and additional visual inspection was performed by comparing the model's predicted bloom regions on SAR imagery with the corresponding ground truth derived from Sentinel-2 data. During the training period, the model achieved a precision of 0.719, indicating that approximately 71.9% of the instances identified as algal blooms were correct detections. The recall was 0.914, suggesting that the model successfully identified 91.4% of actual algal bloom occurrences. The F1 score, which balances precision and recall, was 0.805, reflecting a strong overall performance. During the testing period, the precision for the test dataset was determined to be 0.600, indicating that 60% of the predicted positive instances were true positives. The recall for the test dataset was 0.692, suggesting that the model identified 69% of the actual instances of algal blooms, resulting in a certain number of false negatives. To mitigate false predictions, we refined the classification threshold to balance precision and recall, enhanced the training dataset with diverse scenarios, applied data augmentation techniques to increase variability. These strategies contributed to a more robust model with improved predictive performance. Then, the F1 score was identified to be 0.643, suggesting that the model can be a promising tool for an early prediction of the algal bloom outbreak with a room of improvement (S. Lee and Lee 2018). Furthermore, Gao et al. (2022) also stated the precision for detecting the algae bloom through SAR imagery to be 0.600, with a different type of model. Our model demonstrates the potential for real-world applications in early algal bloom detection systems. However, it is important to acknowledge that the evaluation of our model, relying on Sentinel-2 for visual inspection, presents certain limitations. The reliance on optical imagery for validation might introduce subjective interpretation and may not fully capture the dynamics of algal bloom events under various environmental conditions. As suggested by Colkesen, Ozturk, and Altuntas (2024), incorporating indices such as the Floating Algae Index (FAI) and Surface Algal Blooms Index (SABI) could improve the accuracy and robustness of detection systems, providing a more comprehensive validation of SAR-based models in future studies.

### 3.3. Applications of the algal bloom detection model

#### 3.3.1. Seasonal patterns of algal bloom occurrences and their suggestions for proactive management

For a comprehensive understanding of algal blooms, we applied the developed model to find the algal

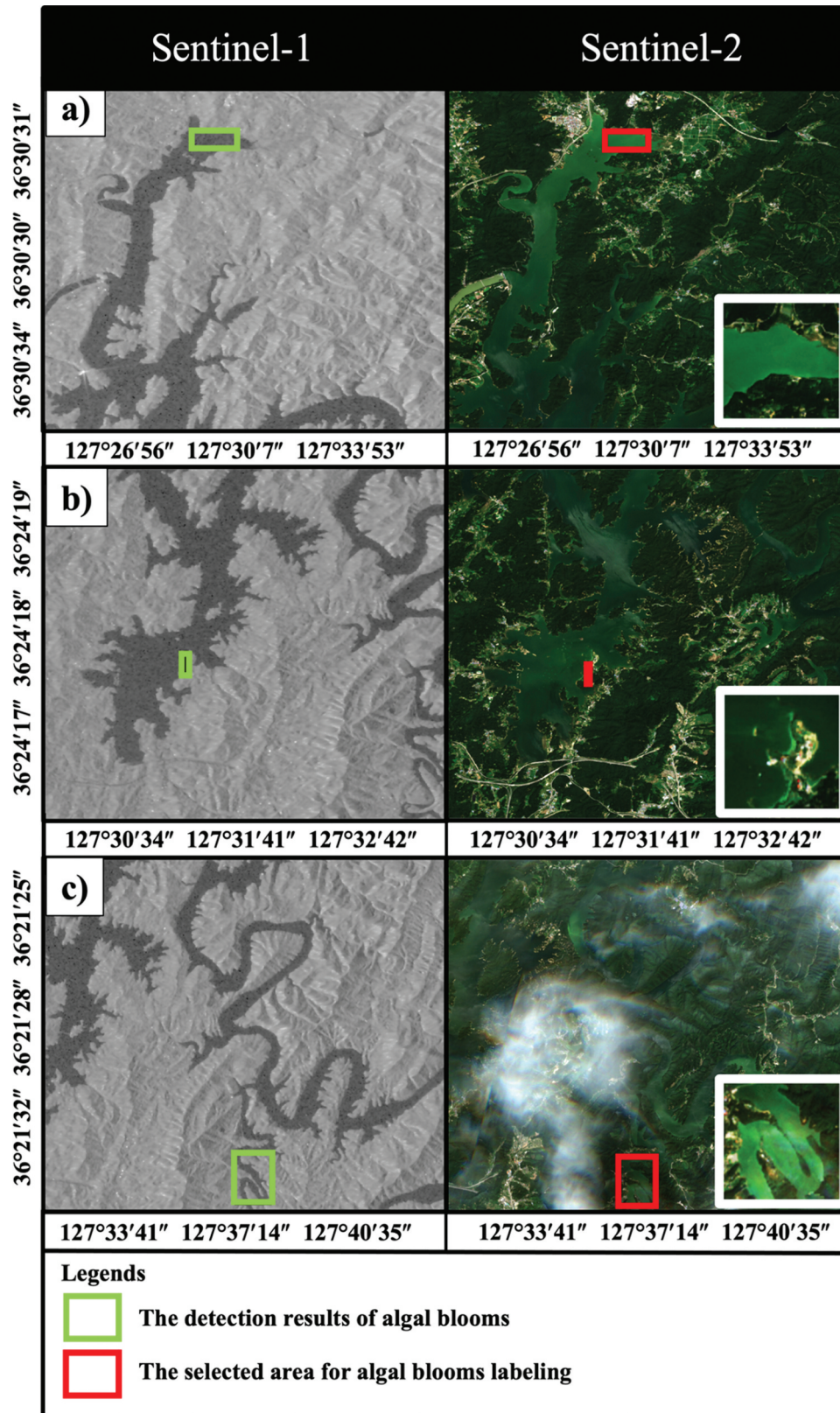


**Figure 6.** Algal detection results were selected from the developed Faster R-CNN model and represented the area located in the GR basin. Each subfigure consists of Sentinel-1 imagery on the left, showing the model-predicted algal bloom areas (green boxes), and the corresponding Sentinel-2 RGB composite on the right serving as visual reference. Red boxes highlight the observed bloom locations based on optical interpretation; (a) Mooni is territorial waters from Daecheong Reservoir located in the north-western direction on August 25, 2020 (b) Choodong is territorial waters from Daecheong Reservoir located in south-western direction on August 25, 2020 (c) So-oak Cheon is territorial waters from Daecheong Reservoir located at the middle of south direction on September 14, 2022.

**Table 1.** The performance evaluation of the algal bloom detection from the Faster R-CNN model with the best-optimized hyperparameters.

Evaluation Matrices	Training period	Testing period
Precision	0.719	0.600
Recall	0.914	0.692
F1 score	0.805	0.643

bloom outbreak throughout different seasons. The other dataset, which indicates the testing dataset without the training dataset, was simulated with the model for each season at identical locations to analyze the temporal variations in algal bloom occurrences. Figure 7 illustrates distinct variations in algal bloom occurrences observed across seasons. Specifically, from summer 2021 (16 July 2021) to summer 2022 (14 September 2022), the model identified algal blooms only during the summers of 2021 and 2022 in Daecheong Reservoir and the surrounding area known as So-oak Cheon. Interestingly, the model did not detect any algae in the same location from autumn (18 November 2021), winter (17 January 2022), and spring (17 May 2022). The prevalence of algal blooms exhibits fluctuations over the year, influenced by diverse factors including geographical location, weather conditions, and temporal variations (D’Silva et al. 2012). The observed pattern resonates with findings in South Korea, where algal

bloom outbreaks are predominantly observed in the summer months (Y. H. Ahn et al. 2006; Jeong et al. 2022). This aligns with Sentinel-2 imagery, validating that the model was meticulously trained using historical data from the input dataset.

Our study, specifically in the environmental field, even demonstrated the success of Sentinel-1 SAR C-band in detecting algal blooms in rivers characterized by monsoon conditions through the comparison with environmental parameters, demonstrated in Figure S1 (Appendix F). The use of SAR imagery, acting as a time series data source, makes the Faster R-CNN coupled with remote sensing a valuable tool for objective detection and providing initial information for water quality management by identifying algal blooms. Hence, understanding seasonal patterns and predicting outbreaks can lead to a proactive plan.

### 3.3.2. Assessing the efficacy of an algal bloom detection model: case study in South Korea’s algal alert System

NIER has been actively implementing the algal alert system by measuring the cell density of cyanobacteria blooms as an indicator to determine the level of harm, categorized into Caution and Warning levels (Ahn et al. 2003; Ahn et al. 2021; J. H. Kim et al. 2023). The measures

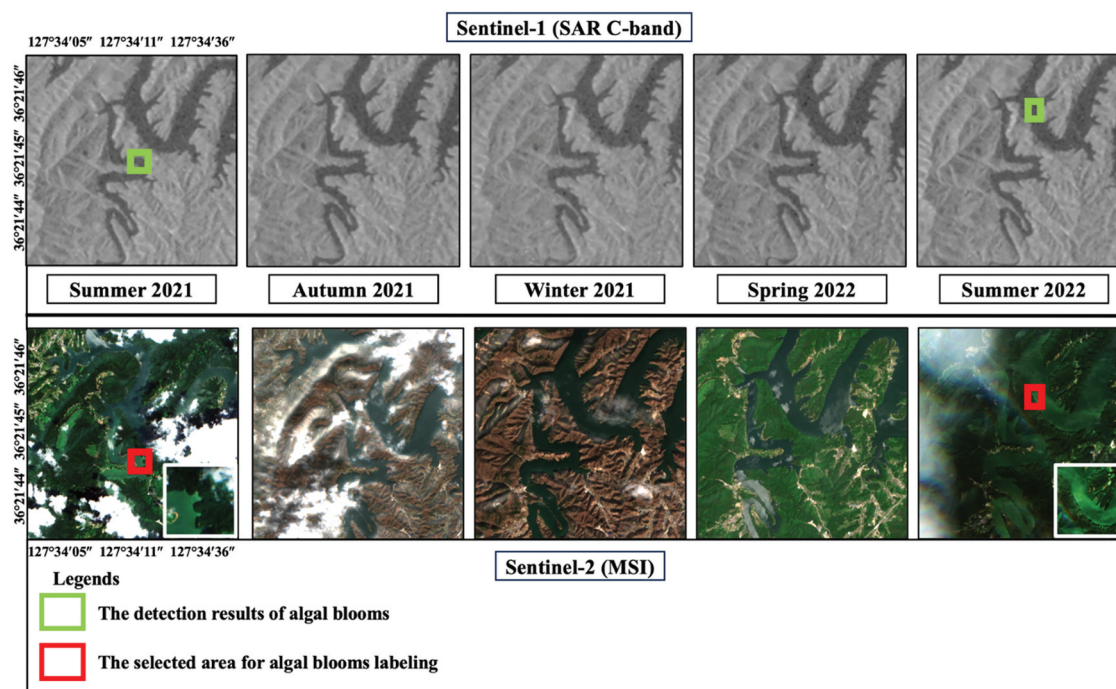


**Figure 7.** The comparison of algal detection results across seasons from summer 2021 (July 16, 2021) to summer 2022 (September 14, 2022) showed the relationship of the captured bounding boxes in summer with the ground truth imagery. The green boxes indicated the auto-generated from the developed model while the red boxes showed the exact location from the ground truth.

were reported annually to ensure a stable supply of tap water and to promote the safety of the public from algae toxins during activities related to water conservation. As illustrated in Figure 7, the model simulation results of the study successfully detected algal blooms in various water sources, particularly in the Daecheong Reservoir. According to NIER's annual reports, instances of algal blooms reaching the Warning level, and requiring serious tracking, were recorded for a total of 90 days in 2020, 69 days in 2021, and 49 days in 2022 in the GR Basin (NIER, <http://211.114.21.27/web>.) (National Institute of Environmental Research 2023). Especially in Figure 7(a), this result aligns with the report, indicating that in 2020 at Mooni, algal blooms occurred from 14 August to 4 October (52 days) and from 16 October to 3 November (19 days). Subsequently, we conducted the simulation on a separate dataset without ground truth or on a dataset obscured by cloud cover, which had not been used during training. Based on the most recent report (version 2022), Figure 8 illustrates algal blooms detected at Mooni from 12 August to 19 October (69 days) in 2021. The detection results align with reported instances of algal blooms reaching Warning levels, as recorded in NIER's annual reports. Despite limited dataset availability due to a typhoon, the model demonstrated its efficiency even under-constrained conditions during the typhoon in August 2021 (Kang et al. 2022). This holds promise for establishing a more stable and reliable system, making it well reflected for integration into the algal bloom alert system.

### 3.4. Implication of the remote sensing of Sentinel-1 for algal blooms detection

Sentinel-1 imagery was proposed to be applied as an input dataset in the deep learning approach for algal bloom detection. In contrast, Sentinel-2 imagery served as the ground truth reference, validating the trustworthiness of the trained model. Although Sentinel-2 imagery has been used as an input dataset in object detection research, it exhibits constraints influenced by weather variability, resulting in fluctuating performance as an input dataset (Fisser et al. 2022). The difficulty comes from the fact that Sentinel-2 imagery relies on optical instruments with apparent optical properties. This property depends on the lights to capture images and the performance can be sensitive to cloud cover or atmospheric conditions. In uncertain weather or nighttime conditions, the optical sensor might fail to provide clear and accurate imagery, adversely affecting deep learning model performance (Meraner et al. 2020). Detection limits have been reported when identifying algae through MSI imagery (Qi and Hu 2021).

On the other hand, Sentinel-1 imagery, operating as an imaging radar satellite, captures reflected signals as it passes over designated areas. The SAR C-band, as a radiofrequency, remains unaffected by atmospheric conditions and clouds due to the ability of microwave radiation to penetrate cloud cover. The SAR C-band's ability to map regions consistently is further augmented by advanced data recording and processing techniques. These techniques combine independent samples

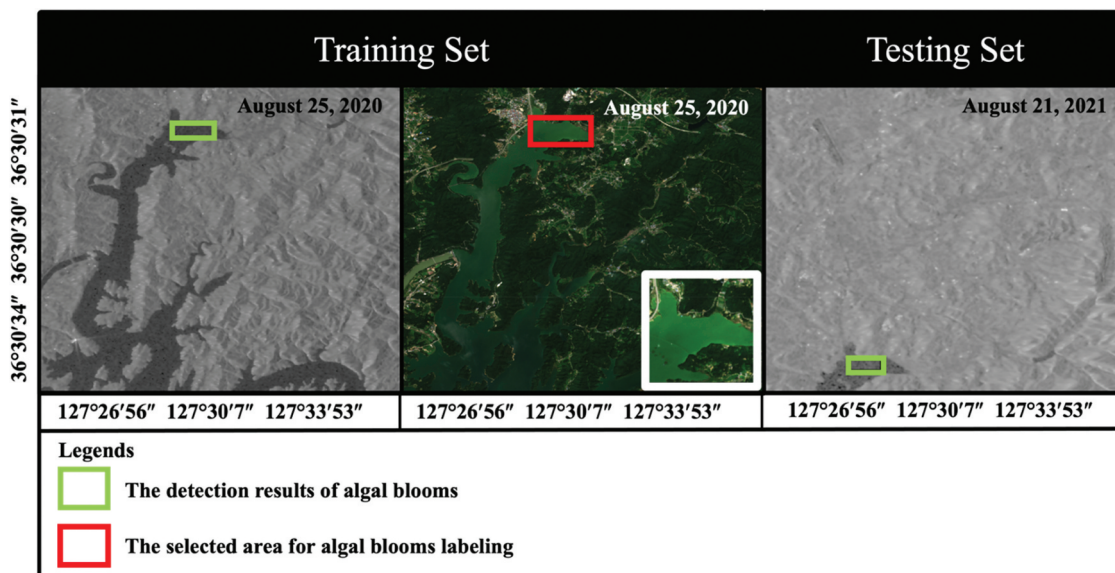


**Figure 8.** The assessing result of the algal bloom detection model in the case study of the algal alert system from the training dataset (August 25, 2020) and testing dataset (August 21, 2021). The model auto-generated green boxes from Sentinel-1 imagery while the red box was created to point to the simulated result in ground truth.

collected from slightly varying positions to generate a single high-resolution SAR image. Thus, SAR C-band technology proves adept at mapping complex regions, making the utilization of imaging radar data more viable, especially in areas where the numbers of data are sparse (Scepanovic et al. 2021).

While Sentinel-2 imagery was used to support model development, as in this study, the intention was not to replace optical-based detection methods. Rather, the SAR-based model is better viewed as a complementary approach that can function effectively when optical data are unavailable or unreliable – such as during cloudy periods, low-light environments, or data acquisition gaps. In this context, the model holds practical value in supporting algal bloom monitoring under challenging environmental conditions that often limit traditional observation methods.

The combined use of Sentinel-1 and Sentinel-2 imagery could significantly enhance the development of a robust early warning algorithm by leveraging multi-modal data (J. Lee. et al. 2025). Sentinel-1 addresses the limitations of multispectral imagery, allowing for continuous and reliable detection and monitoring of algal blooms. Future research could focus on improving the model by integrating both Sentinel-1 and Sentinel-2 as input datasets, particularly in regions with complex environmental conditions, such as fluctuating weather patterns, diverse water turbidity levels, and varying land–water interfaces. Moreover, incorporating complementary data sources, including meteorological and water quality variables from real-time monitoring data, along with multi-modal deep learning approach, could expand the applicability of multiple data sources for water quality management (Kwon et al. 2025). Kwon et al. (2025) showed a multi-modal deep learning that integrated both image data and particle properties to identify harmful algae in the water treatment process, thereby demonstrating that multi-modal learning can conduct a reliable algae identification approach. Also, Sentinel-3 can acquire data in the infrared spectrum, which can be utilized to estimate surface water temperature that is an important variable influencing algal dynamics (Yang et al. 2020). Therefore, further research could incorporate the integration of multiple platforms to more effectively estimate and detect harmful algal blooms for water quality management.

#### 4. Conclusion

We developed a model to identify potential algal bloom areas based on Sentinel-1 SAR imagery, using Sentinel-2-derived reference data as guidance. Algal blooms are currently a major issue in aquatic ecosystems and

require proactive monitoring and regulation. Leveraging the capability of Sentinel-1 to acquire data under all weather conditions, the SAR imagery was integrated with the Faster R-CNN deep learning model to simulate potential bloom outbreaks. The results demonstrate the potential of using SAR imagery in conjunction with deep learning for real-time monitoring and proactive water quality management. The key findings of this study are summarized as follows:

- (1) The sigma naught values of algae in the river were analyzed from SAR imagery, revealing overlapping but statistically distinguishable patterns in sigma naught values among algal blooms, vegetation, and water features. While not conclusive for classification by sigma naught alone, this suggests the potential for further feature-based differentiation.
- (2) SAR imagery was applied to the Faster R-CNN model for algal bloom detection, demonstrating reasonable performance and practical results when evaluated against visually interpreted reference data. The model exhibited a precision of 0.600, a recall of 0.692, and an F1 score of 0.643 during testing, indicating its potential for predicting algal bloom outbreaks.
- (3) The developed model was used to identify the algal bloom outbreak through seasonality. The model shows potential as a supplementary approach to support algal monitoring, particularly when conventional observation methods are unavailable.

This research shows promise in enhancing our understanding of water quality dynamics, especially concerning algal blooms. These significant findings contribute to serve as a complementary tool for monitoring HABs and the basic development of automatic detection algorithms. Given the challenges posed by factors, such as cloud cover and temporal inconsistencies in remote sensing data, this approach can provide a more reliable solution for continuous and effective HAB monitoring, especially in regions with frequent environmental conditions that hinder traditional optical sensing.

Building on these findings, we plan to improve the model by addressing some of the key limitations identified in the review. We aim to gather in-situ data on algal bloom presence or absence, which will provide a more reliable dataset for testing and validating our model. This will help us assess its performance in real-world scenarios. Additionally, we will explore comparisons with other remotely sensed products, such as Sentinel-3A/B imagery, to refine the model's ability to detect algal blooms and better understand the relationship between

various remote sensing data sources, while also focusing on refining spectral index thresholds when using Sentinel-2 imagery to present our results more clearly. These improvements will enhance the model's accuracy and support more effective monitoring of algal blooms, ultimately helping with better water quality management and ecosystem protection.

## Author contributions

**Kritnipit Phetanan:** Writing – Original Draft, Methodology, Formal analysis, Visualization, Data curation. **Do Hyuck Kwon:** Conceptualization, Methodology, Software, Validation, Writing – Review & Editing, Data curation. **Jinmyeong Lee:** Data curation. **Heewon Jeong:** Data curation. **Gibeom Nam:** Data curation. **Euiho Hwang:** Data curation. **JongCheol Pyo** and **Kyung Hwa Cho:** Supervision, Project administration.

## Disclosure statement

No potential conflict of interest was reported by the author(s).

## Funding

This research was supported by a National Research Foundation of Korea grant from the Korean Government (Ministry of Science and ICT—MSIT) [RS-2025-24683148]. Also, this research was partially supported by Ministry of Environment, under the Development of Ground Operation System for Water Resources Satellite from K-water.

## Data availability statement

The data that support the findings of this study are available from the corresponding author, K.H. Cho, upon reasonable request.

## References

- Adamo, M., E. Matta, M. Bresciani, G. De Carolis, D. Vaiciute, C. Giardino, and G. Pasquariello. 2013. "On the Synergistic Use of SAR and Optical Imagery to Monitor Cyanobacteria Blooms: The Curonian Lagoon Case Study." *European Journal of Remote Sensing* 46 (1): 789–805. <https://doi.org/10.5721/EuJRS20134647>.
- Adams, J. B., M. O. Smith, and P. E. Johnson. 1986. "Spectral Mixture Modeling: A New Analysis of Rock and Soil Types at the Viking Lander 1 Site." *Journal of Geophysical Research Solid Earth* 91 (B8): 8098–8112. <https://doi.org/10.1029/JB091iB08p08098>.
- Ahn, C. Y., H. S. Kim, B. D. Yoon, and H. M. Oh. 2003. "Influence of Rainfall on Cyanobacterial Bloom in Daechung Reservoir." *Korean Journal of Ecology and Environment* 36:4 413–419.
- Ahn, J. M., J. Kim, L. J. Park, J. Jeon, J. Jong, J. H. Min, and T. Kang. 2021. "Predicting Cyanobacterial Harmful Algal Blooms (Cyanohabs) in a Regulated River Using a Revised Efdc Model." *Water (Switzerland)* 13 (4): 439. <https://doi.org/10.3390/w13040439>.
- Ahn, Y. H., P. Shanmugam, J. H. Ryu, and J. C. Jeong. 2006. "Satellite Detection of Harmful Algal Bloom Occurrences in Korean Waters." *Harmful Algae* 5 (2): 213–231. <https://doi.org/10.1016/j.hal.2005.07.007>.
- Alibrahim, H., and S. A. Ludwig. 2021. "Hyperparameter Optimization: Comparing Genetic Algorithm Against Grid Search and Bayesian Optimization." In *2021 IEEE Congress on Evolutionary Computation, CEC 2021 - Proceedings*, 1551–1559. Kraków, Poland: Institute of Electrical and Electronics Engineers Inc. <https://doi.org/10.1109/CEC45853.2021.9504761>.
- Back, S., J. Park, and J. Park. 2015. "Modeling for Estimation of Algal Bloom in Daecheong Lake Using the Satellite Imagery." *International Conference on Environmental Engineering and Remote Sensing*, 101–105. Phuket, Thailand: Atlantis Press. <https://doi.org/10.2991/eers-15.2015.25>.
- Baek, S. S., E. Y. Jung, J. C. Pyo, Y. Pachepsky, H. Son, and K. H. Cho. 2022. "Hierarchical Deep Learning Model to Simulate Phytoplankton at Phylum/Class and Genus Levels and Zooplankton at the Genus Level." *Water Research* 218:118494. <https://doi.org/10.1016/j.watres.2022.118494>.
- Bergstra, J., J. B. Ca, and Y. B. Ca. 2012. "Random Search for hyper-Parameter Optimization Yoshua Bengio." *Journal of Machine Learning Research* 13 (10): 281–305.
- Brooks, B. W., J. M. Lazorchak, M. D. A. Howard, M. V. Johnson, S. L. Morton, D. A. K. Perkins, E. D. Reavie, G. I. Scott, S. A. Smith, and J. A. Steevens. 2016. "Are Harmful Algal Blooms Becoming the Greatest Inland Water Quality Threat to Public Health and Aquatic Ecosystems?" *Environmental Toxicology and Chemistry* 35 (1): 6–13. <https://doi.org/10.1002/etc.3220>.
- Chai, B., L. Chen, H. Shi, and C. He. 2021. "Marine Ship Detection Method for SAR Image Based on Improved Faster RCNN." *2021 SAR in Big Data Era (BIGSAR DATA)*, 1–4. Nanjing, China: IEEE. <https://doi.org/10.1109/BIGSAR DATA53212.2021.9574162>.
- Colkesen, I., M. Y. Ozturk, and O. Y. Altuntas. 2024. "Comparative Evaluation of Performances of Algae Indices, Pixel- and Object-Based Machine Learning Algorithms in Mapping Floating Algal Blooms Using Sentinel-2 Imagery." *Stochastic Environmental Research and Risk Assessment* 38 (4): 1613–1634. <https://doi.org/10.1007/s00477-023-02648-1>.
- Cook, K. V., J. E. Beyer, X. Xiao, and K. D. Hambright. 2023. "Ground-Based Remote Sensing Provides Alternative to Satellites for Monitoring Cyanobacteria in Small Lakes." *Water Research* 242:120076. <https://doi.org/10.1016/j.watres.2023.120076>.
- D'Silva, M. S., A. C. Anil, R. K. Naik, and P. M. D'Costa. 2012. "Algal Blooms: A Perspective from the Coasts of India." *Natural Hazards* 63 (2): 1225–1253. <https://doi.org/10.1007/s11069-012-0190-9>.
- Ecosystem, C.D.S.C.D.S. 2023. "Copernicus Data Space Ecosystem - Europe's Eyes on Earth [WWW Document]. Accessed October 10, 24. <https://dataspace.copernicus.eu/>.
- ESA (European Space Agency). 2013. "sentinel-2 User Handbook Sentinel-2 User Handbook sentinel-2 User Handbook Title Sentinel-2 User Handbook Issue 1 Revision 1 sentinel-2 User Handbook."
- Evora, N. D., and P. Coulibaly. 2009. "Recent Advances in data-Driven Modeling of Remote Sensing Applications in

- Hydrology." *Journal of Hydroinformatics* 11 (3–4): 194–201. <https://doi.org/10.2166/hydro.2009.036>.
- Fang, F., L. Li, H. Zhu, and J.-H. Lim. 2020. "Combining Faster R-Cnn and Model-Driven Clustering for Elongated Object Detection." *IEEE Transactions on Image Processing* 29:2052–2065. <https://doi.org/10.1109/TIP.2019.2947792>.
- Filippini, F. 2019. "Sentinel-1 GRD Preprocessing Workflow." *MDPI Proceedings* 18 (1): 11. <https://doi.org/10.3390/ECRS-3-06201>.
- Fisser, H., E. Khorsandi, M. Wegmann, and F. Baier. 2022. "Detecting Moving Trucks on Roads Using Sentinel-2 Data." *Remote Sensing* 14 (7): 1595. <https://doi.org/10.3390/rs14071595>.
- Fletcher, K., and European Space Agency. 2012. "Sentinel-1: ESA's Radar Observatory Mission for GMES Operational Services." ESA Communications.
- Foster, T., I. Z. Gonçalves, I. Campos, C. M. U. Neale, and N. Brozović. 2019. "Assessing Landscape Scale Heterogeneity in Irrigation Water Use with Remote Sensing and in situ Monitoring." *Environmental Research Letters* 14 (2): 024004. <https://doi.org/10.1088/1748-9326/aaf2be>.
- Gao, L., X. Li, F. Kong, R. Yu, Y. Guo, and Y. Ren. 2022. "Algaenet: A Deep-Learning Framework to Detect Floating Green Algae from Optical and SAR Imagery." *IEEE Journal of Selected Topics in Applied Earth Observations and Remote Sensing* 15:2782–2796. <https://doi.org/10.1109/JSTARS.2022.3162387>.
- Gernez, P., M. L. Zoffoli, T. Lacour, T. H. Fariñas, G. Navarro, I. Caballero, T. Harmel, et al. 2023. "The Many Shades of Red Tides: Sentinel-2 Optical Types of Highly-Concentrated Harmful Algal Blooms." *Remote Sensing of Environment* 287:113486. <https://doi.org/10.1016/j.rse.2023.113486>.
- Girshick, R. 2015. Fast R-CNN. In *2015 IEEE International Conference on Computer Vision (ICCV)*, 1440–1448, Santiago, Chile. <https://doi.org/10.1109/ICCV.2015.169>.
- Goodfellow, I., Y. Bengio, and A. Courville. 2016. *Deep Learning*. MIT Press.
- Hammad Saleem, M., S. Khanchi, J. Potgieter, and K. Mahmood Arif. 2020. "Image-Based Plant Disease Identification by Deep Learning Meta-Architectures." *Plants* 9 (11): 1–23. <https://doi.org/10.3390/plants9111451>.
- Inoue, Y., E. Sakaiya, and C. Wang. 2014. "Capability of C-Band Backscattering Coefficients from High-Resolution Satellite SAR Sensors to Assess Biophysical Variables in Paddy Rice." *Remote Sensing of Environment* 140:257–266. <https://doi.org/10.1016/j.rse.2013.09.001>.
- Jeong, B., M. R. Chapeta, M. Kim, J. Kim, J. Shin, and Y. K. Cha. 2022. "Machine learning-Based Prediction of Harmful Algal Blooms in Water Supply Reservoirs." *Water Quality Research Journal* 57 (4): 304–318. <https://doi.org/10.2166/wqrj.2022.019>.
- Ji, D., S. A. Wells, Z. Yang, D. Liu, Y. Huang, J. Ma, and C. J. Berger. 2017. "Impacts of Water Level Rise on Algal Bloom Prevention in the Tributary of Three Gorges Reservoir, China." *Ecol Eng* 98:70–81. <https://doi.org/10.1016/j.ecoleng.2016.10.019>.
- Jiang, H., and E. Learned-Miller. 2017. "Face Detection with the Faster r-Cnn." In *2017 12th IEEE International Conference on Automatic Face & Gesture Recognition (FG 2017)*, 650–657. Washington, DC, USA.: <https://doi.org/10.1109/FG.2017.82>.
- Jiang, X., and C. Xu. 2022. "Deep Learning and Machine Learning with Grid Search to Predict Later Occurrence of Breast Cancer Metastasis Using Clinical Data." *Journal of Clinical Medicine* 11 (19): 11. <https://doi.org/10.3390/jcm11195772>.
- Jo, H.-W., S. Lee, E. Park, C.-H. Lim, C. Song, H. Lee, Y. Ko, S. Cha, H. Yoon, and W.-K. Lee. 2020. "Deep Learning Applications on Multitemporal SAR (Sentinel-1) Image Classification Using Confined Labeled Data: The Case of Detecting Rice Paddy in South Korea." *IEEE Transactions on Geoscience & Remote Sensing* 58 (11): 7589–7601. <https://doi.org/10.1109/TGRS.2020.2981671>.
- Jung, Y.-Y., D.-C. Koh, Y.-Y. Yoon, H.-I. Kwon, J. Heo, K. Ha, and S.-T. Yun. 2019. "Using Stable Isotopes and Tritium to Delineate Groundwater Flow Systems and Their Relationship to Streams in the Geum River basin, Korea." *Journal of Hydrology (Amst)* 573:267–280. <https://doi.org/10.1016/j.jhydrol.2019.03.084>.
- Junker, M., R. Hoch, and A. Dengel. 1999. "On the Evaluation of Document Analysis Components by Recall, precision, and Accuracy." In *Proceedings of the Fifth International Conference on Document Analysis and Recognition. ICDAR '99 (cat. No.PR00318)*, 713–716. IEEE. <https://doi.org/10.1109/ICDAR.1999.791887>.
- Kang, B., J. Kim, Y. Kwon, J. Choi, Y. Jang, and S. Kwon. 2022. "An Analysis of the Impact of Building Wind by Field Observation in Haeundae LCT Area, South Korea: Typhoon Omais in 2021." *Journal of Ocean Engineering and Technology* 36 (6): 380–389. <https://doi.org/10.26748/ksoe.2022.027>.
- Khan, R. M., B. Salehi, M. Mahdianpari, F. Mohammadimanesh, G. Mountrakis, and L. J. Quackenbush. 2021. "A Meta-Analysis on Harmful Algal Bloom (Hab) Detection and Monitoring: A Remote Sensing Perspective." *Remote Sensing (Basel)* 13 (21): 4347. <https://doi.org/10.3390/rs13214347>.
- Kim, D., H. E. Cho, E. J. Won, H. J. Kim, S. Lee, K. G. An, H. B. Moon, and K. H. Shin. 2022. "Environmental Fate and Trophic Transfer of Synthetic Musk Compounds and Siloxanes in Geum River, Korea: Compound-Specific Nitrogen Isotope Analysis of Amino Acids for Accurate Trophic Position Estimation." *Environment International* 161:161. <https://doi.org/10.1016/j.envint.2022.107123>.
- Kim, H. G., Y. K. Cha, and K. H. Cho. 2024. "Projected Climate Change Impact on Cyanobacterial Bloom Phenology in Temperate Rivers Based on Temperature Dependency." *Water Research* 249:249. <https://doi.org/10.1016/j.watres.2023.120928>.
- Kim, H. S., A. Muhammad, and S. J. Maeng. 2016. *Hydrologic Modeling for Simulation of Rainfall-Runoff at Major Control Points of Geum River Watershed*, 504–512. in: *Procedia Engineering*. Elsevier Ltd. <https://doi.org/10.1016/j.proeng.2016.07.545>.
- Kim, J. H., H. Lee, S. Byeon, J. K. Shin, D. H. Lee, J. Jang, K. Chon, and Y. Park. 2023. "Machine learning-Based Early Warning Level Prediction for Cyanobacterial Blooms Using Environmental Variable Selection and Data Resampling." *Toxics* 11 (12): 955. <https://doi.org/10.3390/toxics11120955>.
- Kim, J., H. Kim, H. Jeon, S. H. Jeong, J. Song, S. K. P. Vadivel, and D. J. Kim. 2021. "Synergistic Use of Geospatial Data for Water Body Extraction from Sentinel-1 Images for Operational Flood Monitoring Across Southeast Asia Using Deep Neural Networks." *Remote Sensing (Basel)* 13 (23): 4759. <https://doi.org/10.3390/rs13234759>.
- Kim, J., H. Kim, K. Kim, and J. M. Ahn. 2023. "Research on the Development and Application of a Deep Learning Model for Effective Management and Response to Harmful Algal Blooms." *Water (Switzerland)* 15 (12): 15. <https://doi.org/10.3390/w15122293>.

- Kim, J., C. Song, S. Lee, H. Jo, E. Park, H. Yu, S. Cha, et al. 2020. "Identifying Potential Vegetation Establishment Areas on the Dried Aral Sea Floor Using Satellite Images." *Land Degradation & Development* 31 (18): 2749–2762. <https://doi.org/10.1002/ldr.3642>.
- Kim, S., M. Kim, H. Kim, S. S. Baek, W. Kim, S. D. Kim, and K. H. Cho. 2022. "Chemical Accidents in Freshwater: Development of Forecasting System for Drinking Water Resources." *Journal of Hazardous Materials* 432:128714. <https://doi.org/10.1016/j.jhazmat.2022.128714>.
- Kim, Y. K., M. Lee, H. S. Song, and S.-W. Lee. 2022. "Automatic Cardiac Arrhythmia Classification Using Residual Network Combined with Long short-Term Memory." *IEEE Transactions on Instrumentation and Measurement* 71:1–17. <https://doi.org/10.1109/TIM.2022.3181276>.
- Krizhevsky, A., I. Sutskever, and G. E. Hinton. 2012. "ImageNet Classification with Deep Convolutional Neural Networks." *Advances in Neural Information Processing Systems* 25 (2): 1097–1105. <https://doi.org/10.1145/3065386>.
- Kwon, D. H., J. M. Ahn, J. C. Pyo, J. Lee, A. Abbas, S. Park, and K. H. Cho. 2025. "Probabilistic Machine Learning-Based Phytoplankton Abundance Using Hyperspectral Remote Sensing." *GIScience and Remote Sensing* 62 (1). <https://doi.org/10.1080/15481603.2025.2484864>.
- Kwon, D. H., S. M. Hong, A. Abbas, S. Park, G. Nam, J. H. Yoo, K. Kim, H. T. Kim, J. C. Pyo, and K. H. Cho. 2023. "Deep learning-Based super-Resolution for Harmful Algal Bloom Monitoring of Inland Water." *GIScience and Remote Sensing* 60 (1): 60. <https://doi.org/10.1080/15481603.2023.2249753>.
- Kwon, D. H., S. M. Hong, A. Abbas, J. Pyo, H. K. Lee, S. S. Baek, and K. H. Cho. 2023. "Inland Harmful Algal Blooms (HABs) Modeling Using Internet of Things (IoT) System and Deep Learning." *Environmental Engineering Research* 28 (1): 210280–0. <https://doi.org/10.4491/eer.2021.280>.
- Kwon, D. H., M. J. Lee, H. Jeong, S. Park, and K. H. Cho. 2025. "Multi-Modal Learning-Based Algae Phyla Identification Using Image and Particle Modalities." *Water Research* 275:123172. <https://doi.org/10.1016/j.watres.2025.123172>.
- Kwon, D. Y., J. Kim, S. Park, and S. Hong. 2023. "Advancements of Remote Data Acquisition and Processing in Unmanned Vehicle Technologies for Water Quality Monitoring: An Extensive Review." *Chemosphere* 343:140198. <https://doi.org/10.1016/j.chemosphere.2023.140198>.
- Lakhmiri, D., S. L. Digabel, and C. Tribes. 2021. "hypernomad: Hyperparameter Optimization of Deep Neural Networks Using Mesh Adaptive Direct Search." *ACM Transactions on Mathematical Software* 47 (3): 1–27. <https://doi.org/10.1145/3450975>.
- Lee, C., H. Kim, and W. O. Kyeong. 2016. "Comparison of Faster R-CNN Models for Object Detection." In *2016 16th International Conference on Control, Automation and Systems (ICCAS)*, 107–110. Gyeongju, Korea (South). <https://doi.org/10.1109/ICCAS.2016.7832305>.
- Lee, J., D. Kwon, H. Jeong, G. Nam, E. Hwang, J. H. Kim, and H. G. Kim. 2025. "Improving Chlorophyll-A Estimation Using Sentinel-2 Data: A Comparative Analysis of Augmented Datasets." *GIScience and Remote Sensing* 62 (1). [10.1080/15481603.2025.2496551](https://doi.org/10.1080/15481603.2025.2496551).
- Lee, S., and D. Lee. 2018. "Improved Prediction of Harmful Algal Blooms in Four Major South Korea's Rivers Using Deep Learning Models." *International Journal of Environmental Research and Public Health* 15 (7): 1322. <https://doi.org/10.3390/ijerph15071322>.
- Lettrache, K., and M. Ramdani. 2023. "Explainable Artificial Intelligence: A Review and Case Study on Model-Agnostic Methods." In *14th International Conference on Intelligent Systems: Theories and Applications (SITA)*, 1–8. Casablanca, Morocco: Institute of Electrical and Electronics Engineers Inc. <https://doi.org/10.1109/SITA60746.2023.10373722>.
- Li, J., C. Qu, and J. Shao. 2017. "Ship Detection in SAR Images Based on an Improved Faster R-CNN." In *2017 SAR in Big Data Era: Models, Methods and Applications (BIGSAR DATA)*, 1–6. Beijing, China: IEEE. <https://doi.org/10.1109/BIGSAR DATA.2017.8124934>.
- Manteaux, S., S. Sauvage, R. Samie, C. Monteil, J. Garnier, V. Thieu, R. Cakir, and J. M. Sánchez-Pérez. 2023. "Modeling in-Stream Biogeochemical Processes at Catchment Scale: Coupling SWAT and RIVE Models." *Environmental Modelling and Software* 170:170. <https://doi.org/10.1016/j.envsoft.2023.105856>.
- Massey, F. J. 1951. "The kolmogorov-Smirnov Test for Goodness of Fit." *Journal of the American Statistical Association* 46 (253): 68. <https://doi.org/10.1080/01621459.1951.10500769>.
- Meraner, A., P. Ebel, X. X. Zhu, and M. Schmitt. 2020. "Cloud Removal in Sentinel-2 Imagery Using a Deep Residual Neural Network and sar-Optical Data Fusion." *ISPRS Journal of Photogrammetry and Remote Sensing* 166:333–346. <https://doi.org/10.1016/j.isprsjprs.2020.05.013>.
- Moeller, H. L., S. Lokas, O. Sy, B. Seitz, and P. Bargellini. 2010. "The GMES-Sentinels Flight Operations Concept." In *SpaceOps 2010 Conference Delivering on the Dream Hosted by NASA Marshall Space Flight Center and Organized by AIAA*, 1924. Alabama, USA. <https://doi.org/10.2514/6.2010-2189>.
- National Institute of Environmental Research. 2023. "Water Environment Information System [WWW Document]. Accessed October 10, 24. <http://211.114.21.27/web>.
- Niculescu, S., J. B. Boissonnat, C. Lardeux, D. Roberts, J. Hanganu, A. Billey, A. Constantinescu, and M. Doroftei. 2020. "Synergy of High-Resolution Radar and Optical Images Satellite for Identification and Mapping of Wetland Macrophytes on the Danube Delta." *Remote Sensing (Basel)* 12 (14): 12. <https://doi.org/10.3390/rs12142188>.
- Park, S. B. 2012. "Algal Blooms Hit South Korean Rivers." *Nature*. <https://doi.org/10.1038/nature.2012.11221>.
- Parmuchi, M. G., H. Karszenbaum, and P. Kandus. 2002. "Mapping Wetlands Using multi-Temporal radarsat-1 Data and a decision-Based Classifier." *Canadian Journal of Remote Sensing* 28 (2): 175–186. <https://doi.org/10.5589/m02-014>.
- Qi, L., and C. Hu. 2021. "To What Extent Can Ulva and Sargassum Be Detected and Separated in Satellite Imagery?" *Harmful Algae* 103:102001. <https://doi.org/10.1016/j.hal.2021.102001>.
- Qian, J., L. Qian, N. Pu, Y. Bi, A. Wilhelms, and S. Norra. 2024. "An Intelligent Early Warning System for Harmful Algal Blooms: Harnessing the Power of Big Data and Deep Learning." *Environmental Science & Technology* 58 (35): 15607–15618. <https://doi.org/10.1021/acs.est.3c03906>.
- Qiu, Y., H. Liu, J. Liu, D. Li, C. Liu, W. Liu, J. Wang, and Y. Jiao. 2023. "A Digital Twin Lake Framework for Monitoring and Management of Harmful Algal Blooms." *Toxins* 15 (11): 665. <https://doi.org/10.3390/toxins15110665>.
- Raj, N., R. Sethunadh, and P. R. Aparna. 2016. "Object Detection in SAR Image Based on Bandlet Transform." *Journal of Visual*

- Communication and Image Representation* 40:376–383. <https://doi.org/10.1016/j.jvcir.2016.07.010>.
- Raven, J. A., and R. J. Geider. 1988. "Temperature and Algal Growth." *New Phytologist* 110 (4): 441–461. <https://doi.org/10.1111/j.1469-8137.1988.tb00282.x>.
- Ren, S., K. He, R. Girshick, and J. Sun. 2015. "Faster r-Cnn: Towards real-Time Object Detection with Region Proposal Networks." *Advances in Neural Information Processing Systems* 28.
- Scepanovic, S., O. Antropov, P. Laurila, Y. Rauste, V. Ignatenko, and J. Praks. 2021. "wide-Area Land Cover Mapping with Sentinel-1 Imagery Using Deep Learning Semantic Segmentation Models." *Selected Topics in Applied Earth Observations and Remote Sensing, IEEE Journal Of* 14:10357–10374. <https://doi.org/10.1109/JSTARS.2021.3116094>.
- Shareef, M. A., A. Toumi, and A. Khenchaf. 2016. "Estimating of Water Quality Parameters using SAR and Thermal Microwave Remote Sensing Data." In *2016 2nd International Conference on Advanced Technologies for Signal and Image Processing (ATSIP) 2016*, March, 586–590. Monastir, Tunisia: IEEE. <https://doi.org/10.1109/ATSIP.2016.7523149>.
- Shim, M. J., S. C. Yoon, and Y. Y. Yoon. 2018. "The Influence of Dam Construction on Water Quality in the Lower Geum River, Korea." *Environmental Quality Management* 28 (2): 113–121. <https://doi.org/10.1002/tqem.21591>.
- Smith, S. L., P.-J. Kindermans, C. Ying, and Q. V. Le. 2017. "Don't Decay the Learning Rate, Increase the Batch Size." arXiv preprint.
- Solomatine, D., L. M. See, and R. J. Abrahart. 2009. "data-Driven Modelling: Concepts, Approaches and Experiences." In *Practical Hydroinformatics*, 17–30. Berlin, Heidelberg: Springer Berlin Heidelberg. [https://doi.org/10.1007/978-3-540-79881-1\\_2](https://doi.org/10.1007/978-3-540-79881-1_2).
- Srivastava, A., C.-Y. Ahn, R. K. Asthana, H.-G. Lee, and H.-M. Oh. 2015. "Status, Alert System, and Prediction of Cyanobacterial Bloom in South Korea." *BioMed Research International* 2015:1–8. <https://doi.org/10.1155/2015/584696>.
- Steinhausen, M. J., P. D. Wagner, B. Narasimhan, and B. Waske. 2018. "Combining Sentinel-1 and Sentinel-2 Data for Improved Land Use and Land Cover Mapping of Monsoon Regions." *International Journal of Applied Earth Observation and Geoinformation* 73:595–604. <https://doi.org/10.1016/j.jag.2018.08.011>.
- Sterner, R. W., and J. P. Grover. 1998. "ALGAL Growth in Warm Temperate Reservoirs: Kinetic Examination of Nitrogen, Temperature, Light, and Other Nutrients." *Water Research* 32 (12): 3539–3548. [https://doi.org/10.1016/S0043-1354\(98\)00165-1](https://doi.org/10.1016/S0043-1354(98)00165-1).
- Sun, X., P. Wu, and S. C. H. Hoi. 2018. "Face Detection Using Deep Learning: An Improved Faster RCNN Approach." *Neurocomputing* 299:42–50. <https://doi.org/10.1016/j.neucom.2018.03.030>.
- Wang, D., F. Zhang, F. Ma, W. Hu, Y. Tang, and Y. Zhou. 2022. "A Benchmark Sentinel-1 SAR Dataset for Airport Detection." *IEEE Journal of Selected Topics in Applied Earth Observations and Remote Sensing* 15:6671–6686. <https://doi.org/10.1109/JSTARS.2022.3192063>.
- Wu, L., M. Sun, L. Min, J. Zhao, N. Li, and Z. Guo. 2019. "An Improved Method of Algal-Bloom Discrimination in Taihu Lake Using Sentinel-1A Data." In *2019 6th Asia-Pacific Conference on Synthetic Aperture Radar (APSAR)*, 1–5. Xiamen: IEEE. <https://doi.org/10.1109/APSAR46974.2019.9048572>.
- Wu, L., L. Wang, L. Min, W. Hou, Z. Guo, J. Zhao, and N. Li. 2018. "Discrimination of Algal-Bloom Using Spaceborne SAR Observations of Great Lakes in China." *Remote Sensing (Basel)* 10 (5): 767. <https://doi.org/10.3390/rs10050767>.
- Yang, J., J. Zhou, F.-M. Götttsche, Z. Long, J. Ma, and R. Luo. 2020. "Investigation and Validation of Algorithms for Estimating Land Surface Temperature from Sentinel-3 SLSTR Data." *International Journal of Applied Earth Observation and Geoinformation* 91:102136. <https://doi.org/10.1016/j.jag.2020.102136>.
- Zhang, H., Y. Cui, Y. Zhang, H. Xu, and F. Li. 2021. "Experimental Study of the Quantitative Impact of Flow Turbulence on Algal Growth." *Water (Switzerland)* 13 (5): 659. <https://doi.org/10.3390/w13050659>.
- Zhang, N., Y. Feng, and E.-J. Lee. 2021. "Activity Object Detection Based on Improved Faster r-Cnn." *Journal of Korea Multimedia Society* 24:416–422. <https://doi.org/10.9717/kmms.2020.24.3.416>.
- Zhang, Z., M. Lu, S. Ji, H. Yu, and C. Nie. 2021. "Rich Cnn Features for Water-Body Segmentation from Very High Resolution Aerial and Satellite Imagery." *Remote Sensing (Basel)* 13 (10): 1912. <https://doi.org/10.3390/rs13101912>.